

Cobalt(II)-Mediated Catalytic Chain Transfer Polymerization of Styrene: Estimating Individual Rate Coefficients via Kinetic Modeling

G. Evan Roberts, Christopher Barner-Kowollik, Thomas P. Davis,* and Johan P. A. Heuts*

Centre for Advanced Macromolecular Design, School of Chemical Engineering and Industrial Chemistry, The University of New South Wales, Sydney, NSW 2052, Australia

Received July 18, 2002; Revised Manuscript Received November 18, 2002

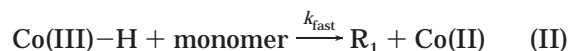
ABSTRACT: The individual rate coefficients for hydrogen abstraction (k_{tr}), cobalt–carbon bond formation (k_{dec}), and cobalt–carbon bond homolysis (k_{ac}) have been determined for the cobaloxime-mediated chain transfer polymerization of styrene at 60 °C using kinetic simulations in combination with experimental data. Values of $2.7 \times 10^6 \text{ L mol}^{-1} \text{ s}^{-1}$, $4.8 \times 10^4 \text{ L mol}^{-1} \text{ s}^{-1}$, and $8.7 \times 10^{-4} \text{ s}^{-1}$ for k_{tr} , k_{dec} , and k_{ac} , respectively, were found to adequately describe reactions associated with the catalytic chain transfer process with the overall model reproducing experimental observations such as molecular weight evolution with time and the initiator concentration dependency of the apparent chain transfer constant. The effect of photolysis of the Co–C bond, leading to an increased free catalyst concentration in the presence of strong UV radiation or a decreased free catalyst concentration under darkened conditions, was modeled by simply varying the value for k_{ac} .

Introduction

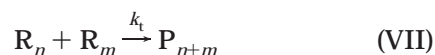
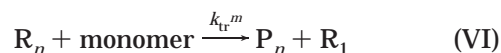
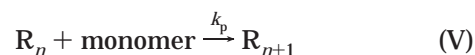
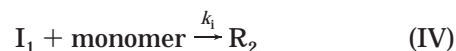
Decades after its initial discovery in the late 1970s,¹ catalytic chain transfer (CCT) using low-spin Co(II) complexes² remains the most efficient way of molecular weight reduction, in both homogeneous^{3–15} and heterogeneous systems.¹⁶ While CCT agents are particularly effective for monomers forming tertiary radicals (such as the methacrylates), their effectiveness as chain transfer agents toward monomers forming secondary radicals (such as the acrylates and styrenics) is reduced.² The major cause of this reduction is the formation of stable cobalt–carbon bonds, effectively reducing the concentration of the active chain transfer agent.^{8,11,14,17–19} Cobalt–carbon bond formation reduces the overall efficiency of the CCTP process for monomers forming secondary radicals, complicating the direct determination of chain transfer rate coefficients. One way of overcoming the obscuring effects of cobalt–carbon bonds is to combine careful experimentation with kinetic modeling.

In a recent paper,²⁰ we demonstrated that the effects of catalyst poisoning in the CCT polymerization of styrene can be substantially reduced by a very thorough purification regime; this allows us to carefully study the kinetics of the reaction to probe rate coefficients. An extended set of experiments were performed over varying conversions and catalyst and initiator concentrations. While it was possible to infer some mechanistic knowledge from these experiments, an enhanced insight can be gained by utilizing mathematical modeling. In this work, kinetic simulations²¹ are used to help probe the CCT polymerization of styrene with COBF. To estimate rate coefficients using this approach, we assume a model and therefore a proviso must be adopted, warning that the derived coefficients and the ensuing discussion rely on the correctness of the assumed model.²¹

The generally accepted mechanism for catalytic chain transfer polymerization, which we use in the current studies, consists of a two-step process involving a Co(III)–H intermediate.^{2,17,22} In the first step (eq I), a growing radical R_n reacts with a Co(II) complex, yielding a dead polymer chain P_n and the Co(III)H intermediate. This step is thought to be rate determining and proceeds with a rate coefficient k_{tr} .



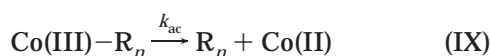
The subsequent reinitiation step (eq II) between a monomer species and the formed Co(III) hydride is considered to be non-rate-determining proceeding with a rate coefficient k_{fast} , yielding a monomeric styryl radical (R_1) and the catalyst in its original state.^{2,17,22} In addition to the CCT process, free-radical polymerization is assumed to proceed via the following set of reaction steps:²¹



Careful ESR and UV–vis experiments on the Co(II)/styrene system have indicated that the extent of cobalt–carbon bond formation in the CCTP of styrene is significant and should not be neglected in a kinetic description of the process.^{17,18,23,24} The reactions associ-

* Authors for correspondence: Fax +61-2-9385 6250; e-mail j.heuts@unsw.edu.au, t.davis@unsw.edu.au.

ated with cobalt carbon bonding may be expressed via the following reaction steps:^{17,18}

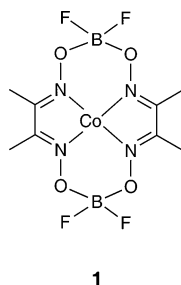


In this proposed mechanism, the cobalt–carbon bond only serves to regulate the concentration of the Co(II) and Co(III)–R species, in which the former is an active CCT agent and the latter is not. Thus, the cobalt–carbon bond formation mechanism is assumed to play no active part in the chain transfer process; i.e., the Co(III)–R cannot undergo a hydrogen transfer reaction to produce Co(III)–H and styrene macromonomer.^{23,25} The deactivation/(re)activation process given by reaction steps VIII and IX is characterized by two rate coefficients: k_{deac} , which governs the Co(II) species deactivation process, and k_{ac} , which governs the (re)activation of active Co(II) from the dormant Co(III)–R_n species. Both rate coefficients may be combined to give the deactivation/activation equilibrium constant, K , given by

$$K = \frac{k_{\text{deac}}}{k_{\text{ac}}} = \frac{[\text{Co(III)}-R_n]}{[\text{Co(II)}][R_n]} \quad (1)$$

The effect of cobalt–carbon bonding on the measured chain transfer constant, C_S^{app} , is potentially dramatic as the true concentration of active catalyst is unknown and a value lower than the true value is obtained.¹⁸

It is the aim of the present study to apply the reaction mechanism described by the reaction steps I–IX to the bis(difluoroboryl)dimethylglyoximatocobalt(II) (COBF, 1)-mediated styrene bulk free radical homopolymeriza-



1

tion at 60 °C and deduce values for the rate coefficients k_{deac} , k_{ac} , and k_{tr} . We aim to do this by using previously reported experimental data²⁰ coupled with the kinetic model represented by reactions steps I–IX using the simulation program PREDICI. Initially, an extensive set of experimental data spanning a wide range of initial COBF and AIBN concentrations are subjected to a parameter estimation procedure for the unknown rate coefficients (i.e., k_{deac} , k_{ac} , and k_{tr}). The second step consists of a thorough sensitivity analysis of k_{deac} and k_{ac} . Finally, further model validation is carried out using the values for k_{deac} , k_{ac} , and k_{tr} obtained via the estimation procedure to predict the dependency of the (apparent) chain transfer constant on the monomer conversion. These predictions are subsequently compared to experimental data.

Procedures

Experiments. The experiments on which the current study is based were reported previously, and a summary of these results can be found in the Supporting Information.²⁰

Table 1. Summary of the Rate Coefficients Used throughout This Work

rate coeff	value ^a	reference
k_{deac}	4.84×10^4	this work
k_{ac}	$8.74 \times 10^{-4} \text{ s}^{-1}$	this work
k_{tr}	2.664×10^6	this work
k_{tr}^{m}	1.70×10^{-2}	39
k_{p}	3.41×10^2	40
k_{ifast}	1.00×10^8	estimate
k_{d}	$6.10 \times 10^{-6} \text{ s}^{-1}$	41, 42
k_{i}	1.50×10^3	estimated at approx 4 times k_{p}
k_{t}	1.00×10^8	43, 44

^a All rate coefficients are given in $\text{L mol}^{-1} \text{ s}^{-1}$ unless otherwise indicated.

Simulations. The parameter estimation procedure to arrive at the rate coefficients k_{ac} , k_{deac} , and k_{tr} and the simulations of molecular weight distributions were carried out on a Pentium III, 733 MHz IBM-compatible computer, equipped with 256 MB RAM and a Windows NT operating system using the program package PREDICI (version 5.36.3) provided by CIT GmbH, Rastede, Germany. The coefficients used for modeling are summarized in Table 1.

Results and Discussion

Estimation of the Rate Coefficients k_{deac} , k_{ac} , and k_{tr} . The most important experimental information necessary for the modeling procedure is the molecular weight evolution with time, $M_w(t)$. The parameter estimation procedure is straightforward and consists of the systematic iteration of k_{deac} , k_{ac} , and k_{tr} in the search for a global minimum in the error space spanned by the three rate coefficients and the sum of errors coordinate generated by comparison with the actual experimental data sets. All rate coefficients governing the reaction steps I–VIII are known from the literature, except the coefficients for steps I, II, VIII, and IX. A summary of the used rate coefficients from the literature and the optimized values for k_{deac} , k_{ac} , and k_{tr} are listed in Table 1.

The validity of the kinetic values obtained by fitting depends on the veracity of the model and the uniqueness of the solution. It is therefore mandatory to plot the sum of errors space that is spanned by the unknown rate coefficients and the sum of errors coordinate. In the case of a four-dimensional problem like the present one, the sum of errors space can only be presented as a cross section with one of the rate coefficients kept constant. Here, we choose to keep k_{tr} constant and investigate the sensitivity of the two other parameters. The reason for this choice is twofold. First, the point estimate for k_{tr} is $2.7 \times 10^6 \text{ L mol}^{-1} \text{ s}^{-1}$, which is in close agreement with the experimental value of $\sim(2-3) \times 10^6 \text{ L mol}^{-1} \text{ s}^{-1}$ and is the least sensitive to experimental changes.^{14,20} Second, the rate coefficients k_{deac} and k_{ac} , which cannot be accessed directly by simple experiments, are the most sensitive to changing experimental conditions. A contour plot of the sum of error space for a fixed k_{tr} is shown in Figure 1. This cross section was generated by using the solution for k_{tr} of $2.7 \times 10^6 \text{ L mol}^{-1} \text{ s}^{-1}$ and varying k_{deac} and k_{ac} systematically computing the sum of errors for each (k_{deac} , k_{ac}) combination. A minimum in the sum of errors surface clearly exists. Although this minimum appears rather extended in the representation given in Figure 1, there is actually a defined minimum point (and not a minimum valley) at the coordinates of ($k_{\text{deac}} = 4.8 \times 10^4 \text{ L mol}^{-1} \text{ s}^{-1}$, $k_{\text{ac}} = 8.7 \times 10^{-4} \text{ s}^{-1}$).

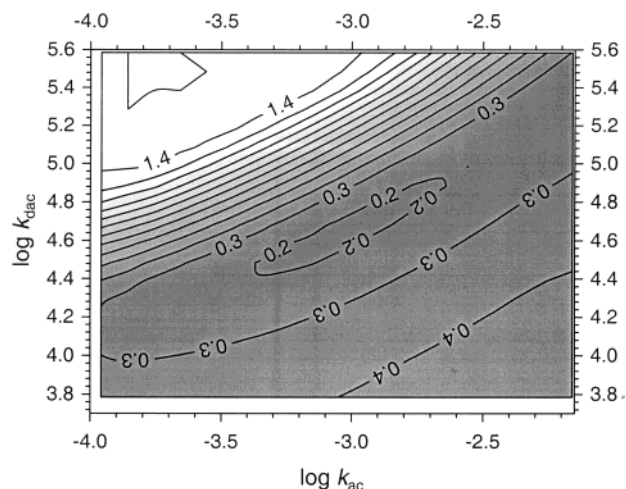


Figure 1. Contour plot of the residuals while holding k_{tr} at $2.66 \times 10^6 \text{ L mol}^{-1} \text{ s}^{-1}$. The figure shows that there is a point solution (where the residual is at a minimum) for this system.

Characteristics of the Catalytic Chain Transfer System. Having established the optimum kinetic parameters for the CCT polymerization of styrene at 60 °C, it is interesting to study some particular aspects of the system in more detail. In particular, we will study the following experimental observations in more detail: (1) The molecular weight is dependent on the concentration of catalyst, conversion, and the concentration of the initiator.^{14,17–20} (2) A corollary of (1) is that the apparent chain transfer constant is dependent on conversion, initiator concentration, and possibly the catalyst concentration. (3) There exists retardation of the initial rate of polymerization and an overall decrease in the rate of polymerization at higher concentrations of the catalyst when compared to rates of polymerization when no catalyst is present.^{14,17,18,20} (4) In the absence of light, the efficiency of the CCT of styrene is considerably diminished.^{14,20}

Molecular Weight Dependency on Kinetic Parameters. In our earlier experimental study,²⁰ we observed that the value for the transfer rate coefficient of COBF with styryl radicals must be at least $2.3 \times 10^6 \text{ L mol}^{-1} \text{ s}^{-1}$ at 60 °C, which is in accordance with the value of $2.7 \times 10^6 \text{ L mol}^{-1} \text{ s}^{-1}$ obtained by the parameter fitting to the model, adding credibility to the adapted modeling procedure. From the activation and deactivation rate parameters, a value of $5.5 \times 10^7 \text{ L mol}^{-1}$ is derived for the overall equilibrium constant K at 60 °C. This value is in good agreement with the published equilibrium constant for the system of tetrakis(*p*-anisyl)-porphyrinatocobalt(II) ((TAP)Co) and styryl radicals at 60 °C ($K = 2.3 \times 10^7 \text{ M}^{-1} \text{ s}^{-1}$)²⁶ but in contrast to what can be inferred from published kinetic data of styryl radicals and cobaloximes (with a variety of axial ligands).²⁷ At given initiator levels (4.4×10^{-4} – $2.4 \times 10^{-2} \text{ mol L}^{-1}$), the steady-state concentration of styryl radicals is estimated in the range $(0.7\text{--}5) \times 10^{-8} \text{ mol L}^{-1}$ (using the proposed model and coefficients from Table 1); thus, at equilibrium the mole fraction of active Co(II) lies between 0.25 and 0.75 (of total cobalt species present), depending on the initiator concentration. In these calculations, only Co(II) and Co(III)–R species are taken into consideration, neglecting any poisoned catalyst or Co(III)–H species. The Co(III)–H species can be neglected because its calculated concentration is insignificant ($\sim 4.5 \times 10^{-16} \text{ mol L}^{-1}$) using the estimated reinitiation rate coefficient of $1 \times 10^8 \text{ L mol}^{-1} \text{ s}^{-1}$.

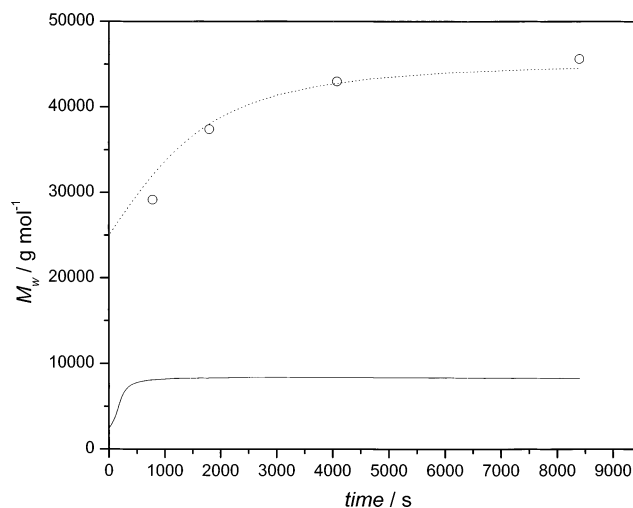


Figure 2. Simulation of the molecular weight evolution using (best fit) equilibrium constants for two dissimilar chain transfer rate coefficients. (○) Experimental data. (···) Line of best fit of experimental data: $k_{tr} = 2.7 \times 10^6 \text{ L mol}^{-1} \text{ s}^{-1}$, $K = 5.5 \times 10^7 \text{ L mol}^{-1}$. (—) Prediction using $k_{tr} = 3 \times 10^7 \text{ L mol}^{-1} \text{ s}^{-1}$ and (best fit) $K = 8 \times 10^8 \text{ L mol}^{-1}$. For all data sets: $[\text{Co}] = 8.36 \times 10^{-6} \text{ mol L}^{-1}$, $[\text{AIBN}] = 2.93 \times 10^{-3} \text{ mol L}^{-1}$, styrene bulk polymerization at 60 °C, and model parameters listed in Table 1.

The obtained chain transfer rate coefficient of $2.7 \times 10^6 \text{ L mol}^{-1} \text{ s}^{-1}$ for the styrene/COBF system is an order of magnitude lower than that found for the MMA/COBF system (i.e., $\sim 3 \times 10^7 \text{ L mol}^{-1} \text{ s}^{-1}$).^{5,7–9,14} As a test of the veracity of this value for styrene, we introduced a chain transfer rate coefficient of 1 order of magnitude higher (i.e., similar to the chain transfer coefficient of MMA/COBF) into the model, and the parameter fitting program was applied to see what equilibrium constant would result. As expected, the value of the equilibrium constant, K , increases so as to decrease the active Co(II), and its point estimate is ~ 15 times higher. It should be noted here, however, that using these parameters only provides an adequate description of some experimental observations and not of others. The main problem lies in the fact that these parameters cannot adequately describe the effect of initiator concentration as was observed experimentally and is discussed in more detail below. An illustrative example is shown in Figure 2, and it is clear that using a chain transfer rate coefficient similar to that in MMA no longer provides a general solution to the model. Therefore, it is evident that the nature of the propagating radical affects the chain transfer rate coefficient, even after accounting for the differences due to cobalt–carbon bonding. In summary, the best fit rate coefficients are $2.7 \times 10^6 \text{ L mol}^{-1} \text{ s}^{-1}$ for the hydrogen abstraction reaction (k_{tr}), $4.8 \times 10^4 \text{ L mol}^{-1} \text{ s}^{-1}$ for the deactivation reaction (k_{deac}), $8.7 \times 10^{-4} \text{ s}^{-1}$ for the (re)activation reaction (k_{ac}), and $5.5 \times 10^7 \text{ L mol}^{-1}$ for the overall equilibrium constant for cobalt–carbon bond formation (K).

It is interesting to investigate the effect of the individual rate coefficients k_{deac} and k_{ac} on $M_w(t)$. Whereas the overall value for K determines the number-average molecular weight after the establishment of the equilibrium, the individual rate coefficients determine the rate at which the equilibrium is established. Since Co(II) is converted into inactive Co(III)–R in this process, k_{ac} and k_{deac} effectively control the evolution of molecular weight with time/conversion. As illustrated by the example in Figure 2, the equilibrium is estab-

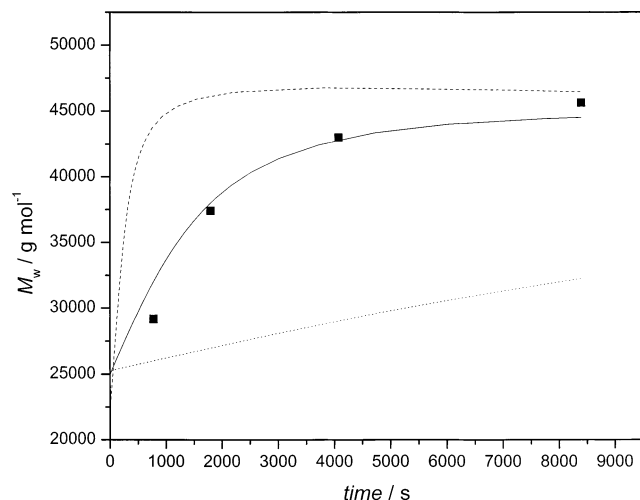


Figure 3. Simulation for the evolution of molecular weight with time as a function of the deactivation reaction rate coefficient. (■) Experimental data. (—) Line of best fit: $k_{\text{deac}} = 4.84 \times 10^4 \text{ mol L}^{-1} \text{ s}^{-1}$ and $K = 5.5 \times 10^7 \text{ L mol}^{-1}$. (---) Model prediction using $k_{\text{deac}} = 4.84 \times 10^5 \text{ mol L}^{-1} \text{ s}^{-1}$ and $K = 5.5 \times 10^7 \text{ L mol}^{-1}$. (···) Model prediction using $k_{\text{deac}} = 4.84 \times 10^3 \text{ mol L}^{-1} \text{ s}^{-1}$ and $K = 5.5 \times 10^7 \text{ L mol}^{-1}$. For all data sets: $[\text{Co}] = 8.36 \times 10^{-6} \text{ mol L}^{-1}$, $[\text{AIBN}] = 2.93 \times 10^{-3} \text{ mol L}^{-1}$, styrene bulk polymerization at 60°C , modeling parameters as listed in Table 1 unless indicated otherwise.

lished relatively slowly in this system, suggesting a low deactivation rate coefficient. Whereas the value of $8.7 \times 10^{-4} \text{ s}^{-1}$ for k_{ac} is of the same order of magnitude as reported for several,^{27,28} but not all,^{26,29} similar systems in the organometallic literature, the value for the deactivation rate coefficient found in the current study is about 3–4 orders of magnitude smaller than those generally reported. Commonly reported values range from about 10^8 to $10^9 \text{ L mol}^{-1} \text{ s}^{-1}$, and the Co–C bond formation process is generally assumed to be diffusion-controlled.^{26,27,28b,29b,30,31} Currently, we cannot explain the discrepancy between these diffusion-controlled values and the value found in the current work. However, we are confident that the low value we find is realistic. A value of $10^8 \text{ L mol}^{-1} \text{ s}^{-1}$ for k_{deac} would lead to a significantly faster established equilibrium, which is clearly not observed experimentally. The effect of k_{deac} on the establishment of the equilibrium is shown in Figure 3; by changing the value of the deactivation rate coefficient while keeping the overall equilibrium constant the same, we can simulate the effect of the value of k_{deac} on the evolution of molecular weight.

It is clear that increasing the deactivation rate coefficient by an order of magnitude hastens the establishment of the equilibrium to such an extent that the simulated evolution of molecular weight no longer accords with experiment. A significant discrepancy also occurs when the deactivation rate coefficient is reduced, and the equilibrium is consequently established too slowly.

Effect of CCT Agent on the Rate of Polymerization. In previous work it was shown that high concentrations of CCT agent have a dramatic effect on the rate of polymerization.^{3,4,7,18} This effect manifests itself in two possible ways. First, the initial rate of polymerization is reduced drastically due to the establishment of the Co(III)–R formation equilibrium which reduces the propagating radical concentration. This effect is most prominently observed in CCT polymerizations of secondary radicals such as styrene and the acry-

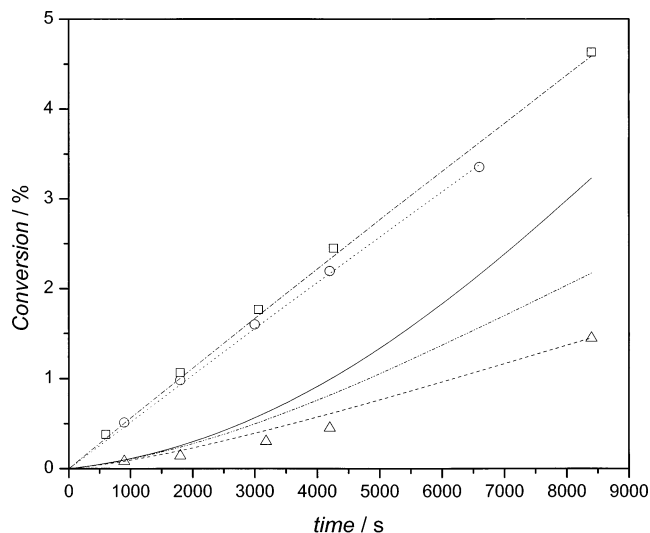


Figure 4. Calculated monomer conversion in a catalytic chain transfer polymerization of styrene in bulk at 60°C as a function of the average termination rate coefficient. (□) Experimental data: $[\text{Co}] = 0 \text{ mol L}^{-1}$, $[\text{AIBN}] = 2.93 \times 10^{-3} \text{ mol L}^{-1}$. (○) Experimental data: $[\text{Co}] = 3.5 \times 10^{-6} \text{ mol L}^{-1}$, $[\text{AIBN}] = 2.93 \times 10^{-3} \text{ mol L}^{-1}$. (△) Experimental data: $[\text{Co}] = 4.5 \times 10^{-4} \text{ mol L}^{-1}$, $[\text{AIBN}] = 2.93 \times 10^{-3} \text{ mol L}^{-1}$. (---) Corresponding model prediction using $\langle k_t \rangle = 1 \times 10^8 \text{ L mol}^{-1} \text{ s}^{-1}$. (···) Corresponding model prediction using $\langle k_t \rangle = 1 \times 10^8 \text{ L mol}^{-1} \text{ s}^{-1}$. (—) Model predictions using $[\text{Co}] = 4.5 \times 10^{-4} \text{ mol L}^{-1}$, $[\text{AIBN}] = 2.93 \times 10^{-3} \text{ mol L}^{-1}$, and $\langle k_t \rangle = 1.1 \times 10^8 \text{ L mol}^{-1} \text{ s}^{-1}$. (— · —) Model predictions using $[\text{Co}] = 4.5 \times 10^{-4} \text{ mol L}^{-1}$, $[\text{AIBN}] = 2.93 \times 10^{-3} \text{ mol L}^{-1}$, and $\langle k_t \rangle = 5 \times 10^8 \text{ L mol}^{-1} \text{ s}^{-1}$.

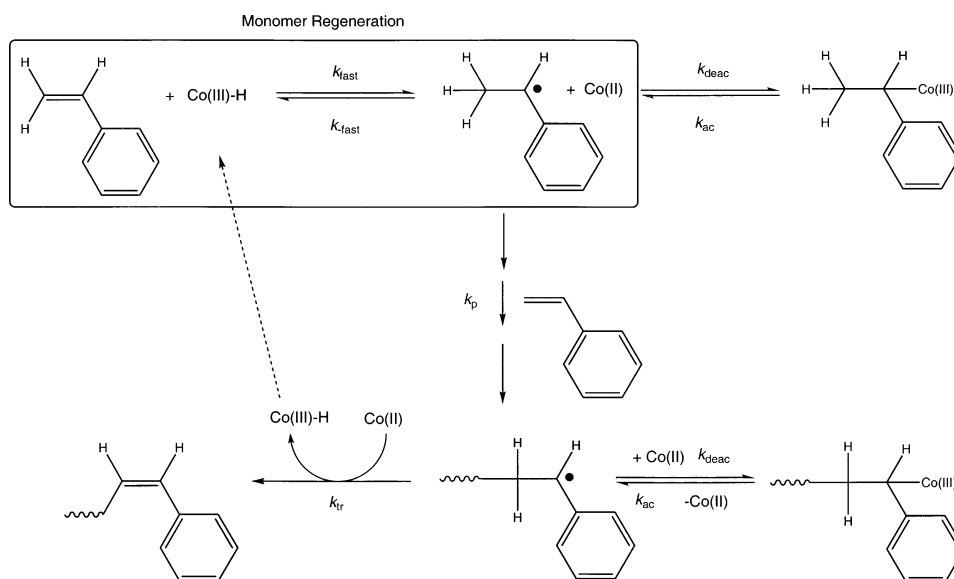
lates.^{11,14,17,18,32} Second, after the establishment of the equilibrium, at which point the propagating radical concentration should equal the steady-state radical concentration and be virtually independent of the added cobalt concentration, still an overall rate reduction is observed. This rate reduction is observed in any type of monomer and has been explained previously in terms of increased termination rates.^{3,7,8} Since we did not include any chain length dependence of the termination rate coefficient in our model, our current model cannot reproduce the rate reduction after the establishment of the Co(III)–R equilibrium, as is clearly shown in Figure 4.

To semiquantitatively investigate the effect of chain length dependent termination, we estimated the chain length averaged termination rate coefficient from the following expression

$$\langle k_t \rangle = k_t^{1,1} \text{DP}_n^{-b} \quad (2)$$

where $k_t^{1,1}$ is the termination rate coefficient for two monomeric radicals and has a value of approximately $10^9 \text{ L mol}^{-1} \text{ s}^{-1}$ and b is a scaling exponent which has a value of 0.5 for center-of-mass diffusion-controlled termination;^{33–35} for $\text{DP}_n \approx 5$, $\langle k_t \rangle \approx 5 \times 10^8 \text{ L mol}^{-1} \text{ s}^{-1}$. It can be seen from Figure 4 that using this higher termination rate coefficient drastically reduces the polymerization rate, but not sufficiently to fit the data; an unrealistically high value of $1.6 \times 10^9 \text{ L mol}^{-1} \text{ s}^{-1}$ would be required to adequately describe the data. Although our treatment of chain length dependent termination is very crude and therefore only approximate, these results further strengthen the previous speculations that an increased termination rate is

Scheme 1



(partly) responsible for the rate reduction at high cobalt concentrations. We did not attempt to further optimize the model because the chain length dependence of the rate coefficients is only important for modeling the production of very short chains (the chain length dependence of $\langle k_t \rangle$ at longer chain lengths is very weak, i.e., $\langle k_t \rangle \propto DP_n^{-0.16}$).^{33–36} To model the situation of very short chains adequately, the chain length dependencies of k_{tr} and k_p would also need to be taken into account, making the model unnecessarily complicated.

A further effect that conceivably causes the polymerization to slow down at high cobalt concentrations is a less efficient overall reinitiation by $Co(III)-H$, as schematically shown in Scheme 1 and explained below.

The first possible reaction is a “reversible” reinitiation between the $Co(III)-H$ and a styrene monomer unit. While the rate coefficient of reinitiation, k_{fast} , is unknown, it has been given an estimate of $1.0 \times 10^8 \text{ L mol}^{-1} \text{ s}^{-1}$ in this work (i.e., the same value as the diffusion-controlled termination rate coefficient k_t). The rate of the reverse reaction, k_{-fast} , is conceivably higher than the nominal value of the transfer rate coefficient, k_{tr} , in a cage effect situation.³⁷ The monomeric radical also offers an α -methyl group for hydrogen atom abstraction, which is absent in longer radicals, which only contain methylene hydrogens suitable for abstraction. The net effect of this process is the fast conversion of a monomeric radical into a monomer molecule rather than the initiation of a growing polymer chain.³⁷

Performance of the Model. The simulated $M_w(t)$ plots using the model and coefficients from Table 1 in combination with the points of four chain transfer constant determination experiments are shown in Figure 5a. These data can be depicted as apparent chain transfer constants as a function of time (and hence monomer conversion) as shown in Figure 5b. The quality of the model is exemplified by a comparison between the simulated and experimental molecular weight distributions in Figure 6, where it can be seen that the discrepancy between the two is insignificant. (The deviation between the calculated and the measured molecular weight distributions is less than the estimated 10% uncertainty of the SEC method.)

In earlier work it was found that the molecular weight at a given catalyst concentration increased in the

absence of light (Table 2),²⁰ which is reflected in the decrease of the apparent chain transfer constant and which is in accordance with experimental observations by Pierik et al. on the same system.^{14,37} In the presence of ambient light (140 min reaction) the apparent C_s is determined to be 4900; when reacted half in light and half in the dark (70 min reaction in light followed by 70 min reaction in the dark), this value decreases to 2700. In the total absence of light (140 min reaction) the apparent chain transfer constant decreases to a value below 1000.

Since the $Co-C$ bond can be broken photochemically,^{30,38} the observed increase in molecular weight under darkened conditions reflects a decrease in the concentration of active $Co(II)$ species. To simulate this effect, the value of k_{ac} was varied, and it was found that experimentally observed molecular weight distributions could be successfully predicted using values for k_{ac} of $8.74 \times 10^{-4} \text{ s}^{-1}$ (light) and $7.74 \times 10^{-5} \text{ s}^{-1}$ (dark) (see Table 2). This qualitative approach predicts both an increase in the weight-average molecular weight and the polydispersity index upon decreasing k_{ac} , in accordance with experimental observations. Furthermore, it predicts that for very high values of k_{ac} , i.e., simulating the presence of strong UV radiation, the apparent C_s asymptotically approaches the real C_s . This principle has been exploited experimentally by Pierik et al.,¹⁴ who used this procedure to measure the real chain transfer constant for styrene at 60 °C and found a value very close to the value we previously determined by decreasing the initiator concentration²⁰ and by the modeling studies described here.

Experimental Errors and Model Limitations. To gain meaningful rate coefficients, experimental error and model limitations must be understood and minimized if possible. Experimental error in the data used for this work is mainly due to the use of SEC to obtain molecular weight distributions (the error is around 5–10%) and weight of catalyst. Weighing of such small quantities of catalyst (i.e., around 0.0015 g for each experiment) has an associated uncertainty of around 13%. The combined error is probably around 20%. (This error is used to calculate the uncertainty in the chain transfer rate coefficient.) To compound these systematic errors, even with the utmost experimental care, random

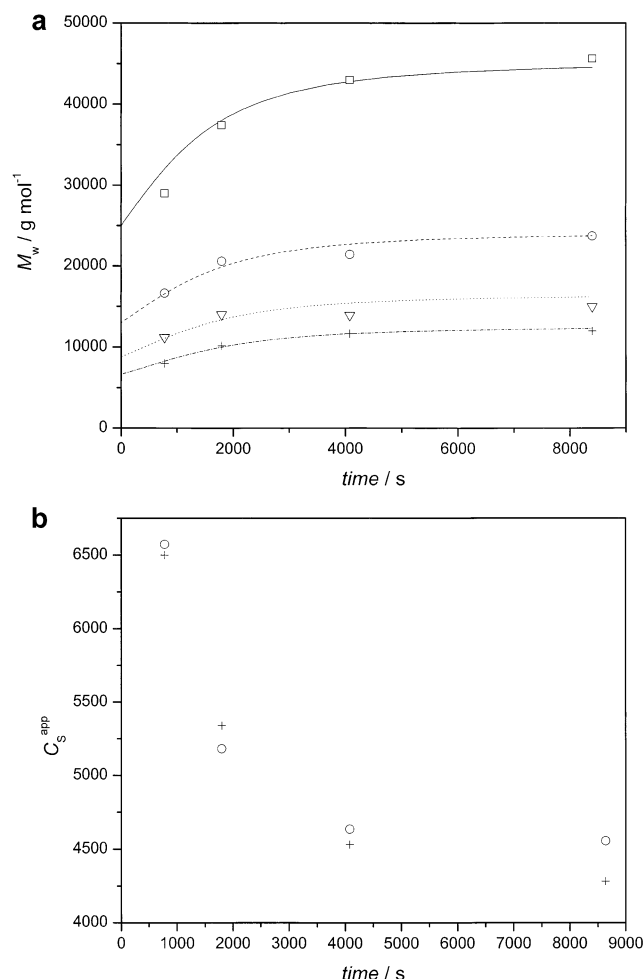


Figure 5. Comparisons of calculated and experimental values for (a) the evolution of weight-average molecular weight with time and (b) the apparent chain transfer constant with conversion in the bulk catalytic chain transfer polymerization of styrene at 60 °C. For all experiments, $[\text{AIBN}] = 2.93 \times 10^{-3} \text{ mol L}^{-1}$. Part a: (\square) experimental data for $[\text{Co}] = 8.36 \times 10^{-6} \text{ mol L}^{-1}$; (—) corresponding simulations; (\circ) $[\text{Co}] = 1.67 \times 10^{-5} \text{ mol L}^{-1}$; (---) corresponding simulations; (∇) experimental data for $[\text{Co}] = 2.51 \times 10^{-5} \text{ mol L}^{-1}$; ($\cdot\cdot\cdot$) corresponding simulations; (+) experimental data for $[\text{Co}] = 3.34 \times 10^{-5} \text{ mol L}^{-1}$; (---) corresponding simulations (sty bulk). Figure b: (\circ) experimental data; (+) simulation results.

errors are always going to be present. Overall, the experimental data are in good agreement with the model predictions, and we refer to the Supporting Information for comparisons of all used experimental molecular weight data with model predictions.

One possible criticism of the model is the lack of incorporation of a chain length dependent average termination rate coefficient. We have shown that the rate of polymerization is dependent on the value used for the average termination rate coefficient; however, the most important experimental parameter used in this modeling (i.e., $M_w(t)$) is not sensitive to the value of the termination rate coefficient used (at least not for the molecular weights generated in this study). Another omission is that there is no allowance for the turnover of monomer in the reinitiation step, but again this will only affect calculations of the conversion, not of the molecular weight produced. Some other reactions have also been left out that may be present but are probably not overly important in the overall scheme. These reactions include transfer to initiator (X), the direct

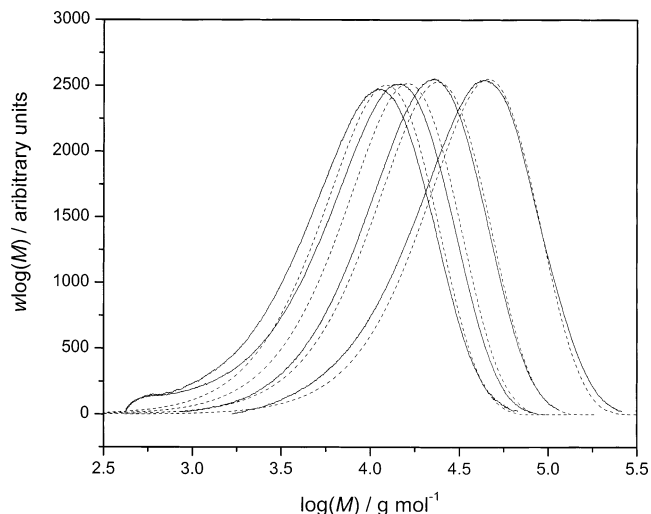
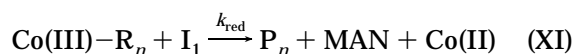
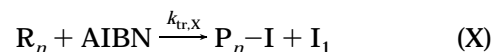


Figure 6. Comparison of full molecular weight distributions obtained via simulation (---) and via experiment using gel permeation chromatography (—) in the bulk catalytic chain transfer polymerization of styrene at 60 °C (same conditions as in Figure 5).

Table 2. Summary of Experimental Results from Light Sensitivity Experiments

experiment	$[\text{Co}]/[\text{Sty}]/10^{-6}$	exptl $M_w/10^3$ g mol^{-1}	PDI	C_s^{app}	predicted $M_w/10^3$ g mol^{-1}
light	1.02	37	1.7	4900	41
	2.04	18	1.9		22
	3.06	13	1.8		15
	4.09	10	1.9		11
$1/2$ light	1.02	65	2.1	2727	
$1/2$ dark	2.04	33	2.0		
	3.06	23	2.1		
	4.09	18	2.5		
dark	1.02	115	2.3	960	116
	2.04	70	2.2		72
	3.06	52	2.4		52
	4.09	44	2.6		41

reduction of the $\text{Co(III)}-\text{R}$ by an initiator fragment (a methacrylonitrile monomeric radical) (XI), and the transfer between a monomeric unit and the catalyst (exhibiting an increased rate of reaction).



We do not believe that these reactions are major features of the overall mechanism.

Conclusions

A model simulation has been described for the catalytic chain transfer of styrene with COBF at 60 °C. This model successfully predicts apparent chain transfer constants as a function of conversion and initiator concentration. The implementation of the model together with experimental data yields a rate coefficient for the hydrogen abstraction by COBF from a propagating styryl radical of $(2.7 \pm 0.3) \times 10^6 \text{ L mol}^{-1} \text{ s}^{-1}$, thus giving a chain transfer constant at 60 °C of ~ 7800 . The overall equilibrium constant, K , for the combination reaction between Co(II) and propagating styryl radicals (R) to give the $\text{Co(III)}-\text{R}$ complex was determined to be $(5.5 \pm 2) \times 10^7 \text{ L mol}^{-1}$, with individual rate

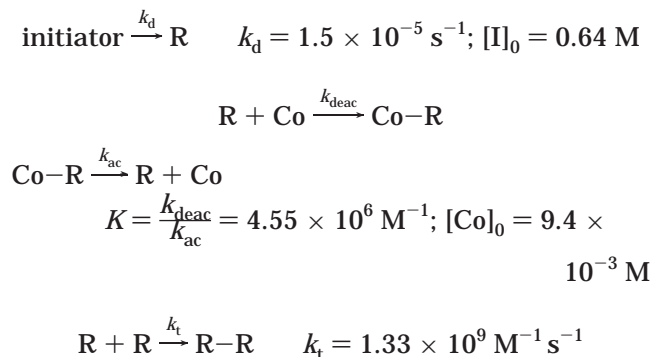
coefficients k_{deac} of $(4.8 \pm 1) \times 10^4 \text{ L mol}^{-1} \text{ s}^{-1}$ and k_{ac} of $(8.7 \pm 1) \times 10^{-4} \text{ s}^{-1}$. It must be stressed that these best-fit coefficients have been determined assuming negligible cobalt catalyst poisoning.

The influence of CCT agent concentration on the rate of polymerization was explained mainly by the chain length dependence of the average termination rate coefficient. In addition, a hypothesis involving cage reactions with Co(II) and monomeric styryl radicals was invoked as a possible explanation for the remaining discrepancy between experiment and simulation including realistic average termination rate coefficients. The effect of light was also examined experimentally, and the observed results could be successfully simulated in a semiquantitative way by varying the value of the (re-)activation rate coefficient.

Acknowledgment. Financial support from the Australian Research Council and Uniqema (ICI) is gratefully acknowledged as are the receipt of an Australian Postgraduate Award to G.E.R. and helpful discussions regarding the sensitivity analysis with Dr. Markus Busch.

Appendix

To further investigate the discrepancy between the value of $4.8 \times 10^4 \text{ L mol}^{-1} \text{ s}^{-1}$ for k_{deac} obtained in the present study and a value of $\sim 10^9 \text{ L mol}^{-1} \text{ s}^{-1}$ generally reported in the organometallic literature, we performed some additional simulations using a simple model. This model was previously used by Woska et al.²⁶ to successfully describe the Co–C bond formation process between (TAP)Co and $\cdot\text{C}(\text{CH}_3)_2\text{CN}$, i.e., the AIBN-derived primary radical, at 60 °C. To be consistent with the nomenclature in the current paper, the used model can be summarized by the following reactions and corresponding kinetic parameters:



Using this simple model and the listed kinetic parameters, the experimental results could be described well. Although no mention is made in this paper regarding the absolute values of k_{ac} and k_{deac} , the reported experimental results are similar to those in an earlier paper in which they report a value of $1.0 \times 10^9 \text{ L mol}^{-1} \text{ s}^{-1}$ for k_{deac} and of 236 s^{-1} for k_{ac} in the same system;^{29a} using a value of $1.0 \times 10^9 \text{ L mol}^{-1} \text{ s}^{-1}$ for k_{deac} in combination with $K = 4.55 \times 10^6 \text{ M}^{-1}$ yields $k_{\text{ac}} = 220 \text{ s}^{-1}$.

In Figure 7 the dependency of the [Co–R] evolution on the individual rate coefficients k_{ac} and k_{deac} is shown, keeping all other parameters in the model constant (closed symbols). The rate coefficient k_{deac} was decreased from 10^9 to $10^4 \text{ L mol}^{-1} \text{ s}^{-1}$ (only 10^9 , 10^7 , and $10^4 \text{ L mol}^{-1} \text{ s}^{-1}$ are shown), with corresponding values for k_{ac} (K was

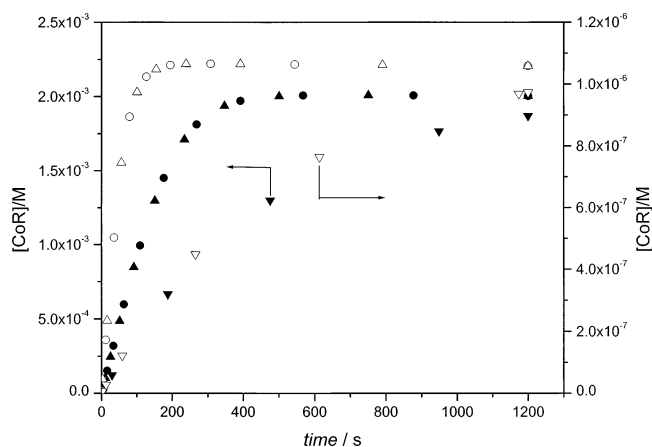


Figure 7. Effect of individual rate coefficients for deactivation and activation on the [Co–R]–time profile for $K = 4.55 \times 10^6 \text{ L mol}^{-1}$; (closed symbols, left axis) $[\text{I}]_0 = 0.64 \text{ M}$ and $[\text{Co}]_0 = 9.4 \times 10^{-3} \text{ M}$; (open symbols, right axis) $[\text{I}]_0 = 1 \times 10^{-3} \text{ M}$ and $[\text{Co}]_0 = 1 \times 10^{-4} \text{ M}$; (●, ○) $k_{\text{deac}} = 10^9 \text{ L mol}^{-1} \text{ s}^{-1}$, $k_{\text{ac}} = 220 \text{ s}^{-1}$; (▲, △) $k_{\text{deac}} = 10^7 \text{ L mol}^{-1} \text{ s}^{-1}$, $k_{\text{ac}} = 2.2 \text{ s}^{-1}$; (▼, ▽) $k_{\text{deac}} = 10^4 \text{ L mol}^{-1} \text{ s}^{-1}$, $k_{\text{ac}} = 2.2 \times 10^{-3} \text{ s}^{-1}$. All data are simulated results using the model and parameter values of k_d and k_t as described in the Appendix.

kept constant), and virtually identical concentration profiles were observed over the range from 10^9 down to $10^6 \text{ L mol}^{-1} \text{ s}^{-1}$. Only below $10^5 \text{ L mol}^{-1} \text{ s}^{-1}$ are significant deviations from the earlier profiles observed. It should be noted here that the experimental results by Woska et al. agree well with the profile obtained for $k_{\text{deac}} = 10^9 \text{ L mol}^{-1} \text{ s}^{-1}$, and hence these results are indeed consistent with their reported experimental values of k_{ac} and k_{deac} . However, it is also clear that both parameters can be decreased by about 3 orders of magnitude to still predict the same concentration, and as such the determination of the equilibrium [Co–R] is probably not sensitive enough to unambiguously determine k_{deac} (and corresponding k_{ac}) if it is not smaller than about $10^5 \text{ L mol}^{-1} \text{ s}^{-1}$. Since values of $\sim 10^9 \text{ L mol}^{-1} \text{ s}^{-1}$ for k_{deac} have also been reported from other, independent, measurements and a value of $10^5 \text{ L mol}^{-1} \text{ s}^{-1}$ does not adequately describe the experimental observation, there are no reasons to assume that any other value than $10^9 \text{ L mol}^{-1} \text{ s}^{-1}$ is required to describe this system. However, this still does not shed any more light on the discrepancy we observe.

To rule out any initial concentration dependence on the profile ($[\text{I}]_0 = 0.64 \text{ M}$ and $[\text{Co}]_0 = 9.4 \times 10^{-3} \text{ M}$ are very high for a typical CCT polymerization), the modeling exercise was repeated for $[\text{I}]_0 = 0.001 \text{ M}$ and $[\text{Co}]_0 = 1.0 \times 10^{-4} \text{ M}$. The results of these simulations (open symbols) are also depicted in Figure 7, and very similar behavior is observed as in the previous case: virtually identical concentration profiles over the range from $k_{\text{deac}} = 10^9$ down to $10^6 \text{ L mol}^{-1} \text{ s}^{-1}$, with significant deviations below $10^5 \text{ L mol}^{-1} \text{ s}^{-1}$. Only the rate and the final equilibrium composition are different.

Finally, we investigated the dependence of the [Co–R] profile on the individual rate parameters using this simple model and the same k_{ac} and k_{deac} as those in Figure 2, with $[\text{I}]_0 = 0.001 \text{ M}$ and $[\text{Co}]_0 = 1.0 \times 10^{-4} \text{ M}$. The results, together with those corresponding to $k_{\text{deac}} = 10^9 \text{ L mol}^{-1} \text{ s}^{-1}$, are shown in Figure 8. It is clear that the observed trend is similar to the trends observed in Figure 7. Furthermore, it is clear that this behavior of [Co–R] is analogous to the behavior of $M_w(t)$ (i.e., $[\text{Co–R}] \uparrow \Rightarrow \text{free } [\text{Co(II)}] \downarrow \Rightarrow M_w \uparrow$), and hence the results

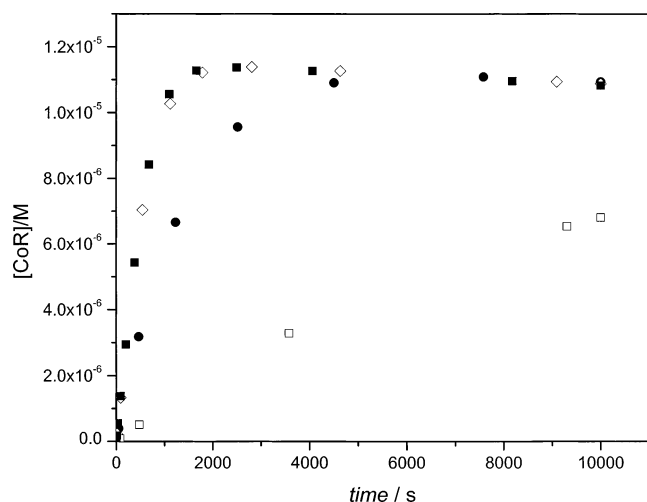


Figure 8. Effect of individual rate coefficients for deactivation and activation on the $[\text{Co-R}]$ -time profile for $K = 5.5 \times 10^7 \text{ L mol}^{-1}$; (●) $k_{\text{deac}} = 4.8 \times 10^4 \text{ L mol}^{-1} \text{ s}^{-1}$, $k_{\text{ac}} = 8.7 \times 10^{-4} \text{ s}^{-1}$; (□) $k_{\text{deac}} = 4.8 \times 10^3 \text{ L mol}^{-1} \text{ s}^{-1}$, $k_{\text{ac}} = 8.7 \times 10^{-5} \text{ s}^{-1}$; (◇) $k_{\text{deac}} = 4.8 \times 10^5 \text{ L mol}^{-1} \text{ s}^{-1}$, $k_{\text{ac}} = 8.7 \times 10^{-3} \text{ s}^{-1}$; (■) $k_{\text{deac}} = 10^9 \text{ L mol}^{-1} \text{ s}^{-1}$, $k_{\text{ac}} = 18 \text{ s}^{-1}$. All data are simulated results using the model and parameter values of k_d and k_t as described in the Appendix.

shown in Figure 8 are in agreement with those shown in Figure 2, ruling out a fortuitous result from the parameter fitting exercise in the current investigations.

From the discussion in this Appendix, it can conceivably be concluded that the results previously described by Wayland and co-workers,^{26,29} and in fact by other workers,^{27,28b,30,31b} on the reaction between Co(II) and a small radical in a nonpolymerizing system cannot be described with a deactivation rate coefficient of less than about $10^5\text{--}10^6 \text{ L mol}^{-1} \text{ s}^{-1}$, whereas our data in the current polymerizing system cannot be described using a deactivation rate coefficient other than about $10^4\text{--}10^5 \text{ L mol}^{-1} \text{ s}^{-1}$. Concluding that the difference is likely to be real, we concede that we cannot think of an explanation at present. Although a possible diffusion argument cannot be ruled out, it is unlikely to explain a difference of 4 orders of magnitude in rate coefficients. (The termination rate coefficient between two long chain polymeric radicals has a value of $\sim 10^7\text{--}10^8 \text{ L mol}^{-1} \text{ s}^{-1}$.)

Supporting Information Available: Table of experimental data used in simulations. This material is available free of charge via the Internet at <http://pubs.acs.org>.

References and Notes

- (1) See, for example: (a) Smirnov, B. R.; Morozova, I. S.; Marchenko, A. P.; Markevich, M. A.; Pushchaeva, L. M.; Enikolopyan, N. S. *Dokl. Akad. Nauk SSSR (Engl. Transl.)* **1980**, *253*, 891. (b) Smirnov, B. R.; Morozova, I. S.; Pushchaeva, L. M.; Marchenko, A. P.; Enikolopyan, N. S. *Dokl. Akad. Nauk SSSR (Engl. Transl.)* **1980**, *255*, 609. (c) Smirnov, B. R.; Marchenko, A. P.; Korolev, G. V.; Bel'govskii, I. M.; Yenikolopyan, N. S. *Polym. Sci. USSR* **1981**, *23*, 1158. (d) Smirnov, B. R.; Plotnikov, V. D.; Ozerkovskii, B. V.; Roshchupkin, V. P.; Yenikolopyan, N. S. *Polym. Sci. USSR* **1981**, *23*, 2807. (e) Enikolopyan, N. S.; Smirnov, B. R.; Ponomarev, G. V.; Bel'govskii, I. M. *J. Polym. Sci., Polym. Chem.* **1981**, *19*, 879.
- (2) For general reviews on catalytic chain transfer polymerization, see: (a) Karmilova, L. V.; Ponomarev, G. V.; Smirnov, B. R.; Bel'govskii, I. M. *Russ. Chem. Rev.* **1984**, *53*, 132. (b) Davis, T. P.; Haddleton, D. M.; Richards, S. N. *J. Macromol. Sci., Rev. Macromol. Chem. Phys.* **1994**, *C34*, 243. (c) Davis, T. P.; Kukulj, D.; Haddleton, D. M.; Maloney, D. R. *Trends Polym. Sci.* **1995**, *3*, 365. (d) Gridnev, A. A. *J. Polym. Sci., Polym. Chem.* **2000**, *38*, 1753. (e) Gridnev, A. A.; Ittel, S. D. *Chem. Rev.* **2001**, *101*, 3611. (f) Heuts, J. P. A.; Roberts, G. E.; Biasutti, J. D. *Aust. J. Chem.* **2002**, *55*, 381.
- (3) Sanayei, R. A.; O'Driscoll, K. F. *J. Macromol. Sci., Chem.* **1989**, *A26*, 1137.
- (4) Gridnev, A. A. *Polym. Sci. USSR* **1989**, *31*, 2369.
- (5) Haddleton, D. M.; Maloney, D. R.; Suddaby, K. G.; Muir, A. V. G.; Richards, S. N. *Macromol. Symp.* **1996**, *111*, 37.
- (6) Krstina, J.; Moad, C. L.; Moad, G.; Rizzardo, E.; Berge, C. T.; Fryd, M. *Macromol. Symp.* **1996**, *111*, 13.
- (7) Suddaby, K. G.; Maloney, D. R.; Haddleton, D. M. *Macromolecules* **1997**, *30*, 702.
- (8) Kukulj, D.; Davis, T. P. *Macromol. Chem. Phys.* **1998**, *199*, 1697.
- (9) Heuts, J. P. A.; Forster, D. J.; Davis, T. P. *Macromolecules* **1999**, *32*, 3907.
- (10) Bon, S. A. F.; Morsley, D. R.; Waterson, J.; Haddleton, D. M.; Lees, M. R.; Horne, T. *Macromol. Symp.* **2001**, *165*, 29.
- (11) Pierik, B.; Masclee, D.; van Herk, A. M. *Macromol. Symp.* **2001**, *165*, 19.
- (12) Haddleton, D. M.; Depaquis, E.; Kelly, E. J.; Kukulj, D.; Morsley, S. R.; Bon, S. A. F.; Eason, M. D.; Steward, A. G. *J. Polym. Sci., Polym. Chem.* **2001**, *39*, 2378.
- (13) Gridnev, A. A. *J. Polym. Sci., Polym. Chem.* **2002**, *40*, 1366.
- (14) Pierik, S. C. J.; Vollmerhaus, R.; Van Herk, A. M.; German, A. L. *Macromol. Symp.* **2002**, *182*, 43.
- (15) Roberts, G. E.; Davis, T. P.; Heuts, J. P. A.; Russell, G. T. *J. Polym. Sci., Polym. Chem.* **2002**, *40*, 782.
- (16) (a) Pashchenko, D. I.; Vinogradova, E. K.; Bel'govskii, I. M.; Ponomarev, G. V.; Enikolopyan, N. S. *Dokl. Akad. Nauk SSSR* **1982**, *265*, 889 (Russian); Chemical Abstracts 98: 4817. (b) Suddaby, K. G.; Haddleton, D. M.; Hastings, J. J.; Richards, S. N.; O'Donnell, J. P. *Macromolecules* **1996**, *29*, 8083. (c) Kukulj, D.; Davis, T. P.; Suddaby, K. G.; Haddleton, D. M.; Gilbert, R. G. *J. Polym. Sci., Polym. Chem.* **1997**, *35*, 859. (d) Kukulj, D.; Davis, T. P.; Gilbert, R. G. *Macromolecules* **1997**, *30*, 7661. (e) Haddleton, D. M.; Morsley, D. R.; O'Donnell, J. P.; Richards, S. N. *J. Polym. Sci., Polym. Chem.* **1999**, *37*, 3549.
- (17) Nokel, A. Y.; Gridnev, A. A.; Mironov, A. F. *Izvestia Vissh. Uchebn. Zaved., Khim. Tekhnol.* **1990**, *33*, 57 (Russian); Chemical Abstracts 113: 132875.
- (18) Heuts, J. P. A.; Forster, D. J.; Davis, T. P.; Yamada, B.; Yamazoe, H.; Azukizawa, M. *Macromolecules* **1999**, *32*, 2511.
- (19) (a) Heuts, J. P. A.; Forster, D. J.; Davis, T. P. In *Transition Metal Catalysis in Macromolecular Design*; Boffa, L. S.; Novak, B. M., Eds.; ACS Symposium Series Vol. 760; American Chemical Society: Washington, DC, 2000; p 254. (b) Heuts, J. P. A.; Forster, D. J.; Davis, T. P. *Polym. Mater. Sci. Eng.* **1999**, *80*, 431.
- (20) Roberts, G. E.; Davis, T. P.; Heuts, J. P. A. *J. Polym. Sci., Polym. Chem.*, in press.
- (21) Kowolik, C.; Davis, T. P. *J. Polym. Sci., Polym. Chem.* **2000**, *38*, 3303.
- (22) Gridnev, A. A.; Ittel, S. D.; Wayland, B. B.; Fryd, M. *Organometallics* **1996**, *15*, 5116.
- (23) Gridnev, A. A.; Ittel, S. D.; Fryd, M.; Wayland, B. B. *Organometallics* **1996**, *15*, 222.
- (24) Gridnev, A. A.; Bel'govskii, I. M.; Enikolopyan, N. S. *Dokl. Akad. Nauk SSSR (Engl. Transl.)* **1986**, *289*, 1408.
- (25) Gridnev, A. A.; Semeikin, A. S.; Koifman, O. I. *Teor. Eksp. Khim.* **1990**, *26*, 128 (Russian); Chemical Abstracts 113: 6862.
- (26) Woska, D. C.; Xie, Z. D.; Gridnev, A. A.; Ittel, S. D.; Fryd, M.; Wayland, B. B. *J. Am. Chem. Soc.* **1996**, *118*, 9102.
- (27) (a) Bakac, A.; Espenson, J. H. *J. Am. Chem. Soc.* **1984**, *106*, 5197. (b) Ng, F. T. T.; Rempel, G. L.; Mancuso, C.; Halpern, J. *Organometallics* **1990**, *9*, 2762.
- (28) (a) Jensen, M. P.; Zinki, D. M.; Halpern, J. *Inorg. Chem.* **1999**, *38*, 2386. (b) Tsou, T.-T.; Loots, M.; Halpern, J. *J. Am. Chem. Soc.* **1982**, *104*, 623.
- (29) (a) Wayland, B. B.; Gridnev, A. A.; Ittel, S. D.; Fryd, M. *Inorg. Chem.* **1994**, *33*, 3830. (b) Woska, D. C.; Wayland, B. B. *Inorg. Chim. Acta* **1998**, *270*, 197.
- (30) (a) Endicott, J. F.; Ferraudi, G. J. *J. Am. Chem. Soc.* **1977**, *99*, 243. (b) Endicott, J. F.; Netzel, T. L. *J. Am. Chem. Soc.* **1979**, *101*, 4000.
- (31) (a) Halpern, J.; Ng, F. T. T.; Rempel, G. L. *J. Am. Chem. Soc.* **1979**, *101*, 7124. (b) Halpern, J. In *Bonding Energetics in Organometallic Compounds*; Marks, T. J., Ed.; ACS Symposium Series Vol. 428; American Chemical Society: Washington, DC, 1990; p 100.

- (32) Roberts, G. E.; Heuts, J. P. A.; Davis, T. P. *Macromolecules* **2000**, *33*, 7765.
- (33) (a) Olaj, O. F.; Zifferer, G.; Gleixner, G.; Stickler, M. *Eur. Polym. J.* **1986**, *22*, 585. (b) Griffiths, M. C.; Strauch, J.; Monteiro, M. J.; Gilbert, R. G. *Macromolecules* **1998**, *31*, 7835.
- (34) See, for example: (a) O'Driscoll, K. F. In *Comprehensive Polymer Science*; Eastmond, G. C., Ledwith, A., Russo, S., Sigwalt, P., Eds.; Pergamon Press: Oxford, 1989; Vol. 3, p 161. (b) Barner-Kowollik, C.; Vana, P.; Davis, T. P. In *Handbook of Radical Polymerization*; Matyjaszewski, K., Davis, T. P., Eds.; Wiley-Interscience: New York, 2002; p 187.
- (35) Smith, G. B.; Russell, G. T.; Heuts, J. P. A. *Macromol. Theory Simul.*, submitted for publication.
- (36) Olaj, O. F.; Vana, P. *Macromol. Rapid Commun.* **1998**, *19*, 433.
- (37) Pierik, S. C. J. Shining a Light on Catalytic Chain Transfer (thesis). Ph.D. Thesis, Technische Universiteit Eindhoven, 2002.
- (38) See, for example: (a) Avranitopoulos, L. D.; Greuel, M. P.; King, B. M.; Shim, A. K.; Harwood, H. J. In *Controlled Radical Polymerization*; Matyjaszewski, K., Ed.; ACS Symposium Series Vol. 685; American Chemical Society: Washington, DC, 1998; p 316. (b) Schrauzer, G. N.; Lee, L. P.; Sibert, J. W. *J. Am. Chem. Soc.* **1970**, *92*, 2997. (c) Brown, K. L.; Zou, X. *Inorg. Chem.* **1992**, *31*, 2541.
- (39) Tobolsky, A. V.; Offenbach, J. *J. Polym. Sci.* **1955**, *16*, 311.
- (40) Buback, M.; Gilbert, R. G.; Hutchinson, R. A.; Klumperman, B.; Kuchta, F.-D.; Manders, B. G.; O'Driscoll, K. F.; Russell, G. T.; Schweer, J. *Macromol. Chem. Phys.* **1995**, *196*, 3267.
- (41) Buback, M.; Huckestein, B.; Kuchta, F.-D.; Russell, G. T.; Schmid, E. *Macromol. Chem. Phys.* **1994**, *195*, 2117.
- (42) Moad, G.; Rizzardo, E.; Solomon, D. H.; Johns, S. R.; Willing, R. I. *Makromol. Chem. Rapid Commun.* **1984**, *5*, 793.
- (43) Buback, M. In *Controlled/Living Radical Polymerization*; Matyjaszewski, K., Ed.; ACS Symposium Series Vol. 768; American Chemical Society: Washington, DC, 2000; p 39.
- (44) Beuermann, S.; Buback, M. *Prog. Polym. Sci.* **2002**, *27*, 191.

MA021152C